

Structure and properties of laser alloyed gradient surface layers of the hot-work tool steels

L.A. Dobrzański*, M. Bonek, E. Hajduczek, K. Labisz, M. Piec, E. Jonda, A. Polok
Division of Materials Processing Technology, Management and Computer Techniques
in Materials Science, Institute of Engineering Materials and Biomaterials,
Silesian University of Technology, ul. Konarskiego 18a, 44-100 Gliwice, Poland
* Corresponding author: E-mail address: leszek.dobrzanski@polsl.pl

Received 16.09.2008; published in revised form 01.12.2008

Manufacturing and processing

ABSTRACT

Purpose: The purpose of this research paper is focused on the 55NiCrMoV7, 32CrMoV12-28, X40CrMoV5-1, X38CrMoV5-3 hot work tool steels surface layers improvement properties using HPDL laser. The paper present laser surface technologies, investigation of structure and properties of the hot work tool steels alloying with ceramic particles using high power diode laser HPDL.

Design/methodology/approach: Investigation indicate the influence of the alloying carbides on the structure and properties of the surface layer of investigated steel depending on the kind of alloying carbides and power implemented laser (HPDL). Laser alloying of surface layer of investigated steel without introducing alloying additions into liquid molten metal pool, in the whole range of used laser power, causes size reduction of dendritic microstructure with the direction of crystallization consistent with the direction of heat carrying away from the zone of impact of laser beam.

Findings: In the effect of laser alloying with powders of carbides NbC, TaC, TiC, WC and VC occurs size reduction of microstructure as well as dispersion hardening through fused in but partially dissolved carbides and consolidation through enrichment of surface layer in alloying additions coming from dissolving carbides. Introduced particles of carbides and in part remain undissolved, creating conglomerates being a result of fusion of undissolved powder grains into molten metal base. In effect of convection movements of material in the liquid state, conglomerates of carbides arrange themselves in the characteristic of swirl. Remelting of the steel without introducing into liquid molten pool the alloying additions in the form of carbide powders, causes slight increase of properties of surface layer of investigated steel in comparison to its analogical properties obtained through conventional heat treatment, depending on the laser beam power implemented for remelting.

Practical implications: It has the important cognitive significance and gives grounds to the practical employment of these technologies for forming the surfaces of new tools and regeneration of the used ones. The increase of hardness of surface layer obtained throughout remelting and alloying with carbides by high power diode laser is accompanied by increase of tribological properties, when comparing to the steel processed with conventional heat treatment.

Originality/value: The outcome of the research is an investigation and proving the structural mechanisms accompanying laser remelting and alloying. The artificial neural networks were used to determine the effect of the technological effect of laser alloying on hardness and resistance wear abrasion of the hot work tool steels.

Keywords: Heat treatment; Laser; Tool materials

1. Introduction

Laser surface treatment technologies feature one of the long-range manufacturing methods of the highly resistant gradient layers on the alloy tool steels. Laser enrichment of the surface layer with the alloy additions belongs to the unconventional surface heat treatment of materials nowadays [1-4]. The nature of this process is quick heating of the processed element's surface, necessary for inducing the phase transformation, putting down the suitable coating or fusion penetration of the selected elements and powders of the hard phases [5-16]. Thanks to the very fast heating up succeeded by cooling the surface properties are obtained that could not be attained with other conventional methods. The laser technologies used most often include alloying, fusion penetration, and remelting, which provide the highest quality surface coatings with thickness of 0.1-1.5 mm and very high quality adhesion with the substrate which can be used for the significant part of tools made with tolerance below 0.1-0.5 mm, when the progressive flank wear tool life criterion does not exceed 0.1-0.5 mm. Gradient layers made with the laser technique, apart from the very good metallurgical joint with the substrate, provide high corrosion resistance, abrasive wear resistance, high heat resistance and hardness, as well as ductility, plasticity and fatigue resistance, which are difficult or even impossible to obtain with other technologies [7,17-22]. The world industry widely uses currently the laser technologies and the most extensive industrial use in the laser materials processing have the solid state lasers with the Nd:YAG crystal active element and the CO₂ gas lasers. Research carried out currently here and abroad by specialists in the laser technologies are focused on the classic technologies of laser surface treatment, laser alloying and cladding mostly for the high-speed- and machine steels using these laser types [17-33]. The dynamical development of laser techniques and devices resulted in introduction to the industry of the high power diode lasers, which provides chances of further development and significant extension of the surface engineering technology applications and also alloying and laser cladding, as well as applying this unique laser for modification of surface layers, and especially for forming the gradient layers. The base of laser treatment are operations that use the laser radiation beam as the energy source needed for heating up the material surface layer to change its structure, attain the suitable mechanical-, physical-, or chemical properties extending the treated element's service life. Remelting of the thin surface layer and its quick recrystallization make it possible to obtain the chemically homogeneous, fine-crystalline, with the particular texture and characteristic of a high hardness. It is important that one can concentrate the laser radiation beam to the very small dimension, even as small as a portion of a micrometer. This promotes obtaining the extremely big power concentration values and selective acting with the beam on the carefully selected material areas, in the hard to access locations, subjected to mechanical loads, etc., with no fear of the effect of the delivered heat on the adjacent areas, neighbouring elements and deformation of the treated elements. Very short time and high energy delivered to the treatment location make it possible to execute the process excluding burning, minimization of chemical impurities, and elimination of the oxidation process[3, 9-13].

Research projects in the area of using laser techniques for constituting the gradient surface layers are the consequent

continuation of the many years long research carried out in the Institute of Engineering Materials and Biomaterials, and employing the methodology of laser alloying of gradient layers features the contemporary approach to the problem of the additional improvement of hardness and abrasion wear resistance of the modern tools with the simultaneous reduction of their manufacturing costs [17-33]. The proposed technology of obtaining the gradient layers may be used in manufacturing and regeneration processes of tools like mill rolls and rollers made from steel, cast steel, and alloy cast iron, and especially of the continuous steel casting installation rolls, dies, forging punches and blanking tools, and cutting tools.

2. Material for investigation

Investigations were carried out on test pieces from the 55NiCrMoV7, 32CrMoV12-28, X40CrMoV5-1 and X38CrMoV5-3 hot work high-speed tool steels with the compositions according to PN-EN ISO 4957:2004 standard. Chemical composition of the steels are given in Table 1. The investigated steel were molten in the electric vacuum furnace at the pressure of about 1 Pa, cast into ingots weighing about 250 kg, and were roughed at the temperature range 1100-900°C into the O.D. 76 mm bars 3 m long, which were soft annealed. Test pieces were machined for structural, tribological, and heat fatigue tests, of the following dimensions: 65 x 25 x 5 mm, Ø70 x 5 mm. Specimens prepared like that were subjected to heat treatment consisting in quenching and tempering twice. Austenitizing was carried out in vacuum furnace at temperature of 850°C for 30 min for the 55NiCrMoV7 steel, at temperature of 1020°C for 15 min for the X40CrMoV5-1 steel, and at temperature of 1060°C for 30 min for the 32CrMoV12-28 and X38CrMoV5-3 steels. Two isothermal holds were used during heating up to the austenitizing temperature, at the temperatures of 585 °C and 850 °C. The specimens were tempered twice after quenching, each time for 2 hours, at the temperatures of 600°C and 550 °C for the 55NiCrMoV7 steel; 550°C and 510°C for the 32CrMoV12-28 steel; 560°C and 510°C for the X40CrMoV5-1 steel, and 575°C and 560°C for the X38CrMoV5-3 steel. Surfaces of specimens were ground on magnetic grinder after heat treatment. Particular attention was paid to prevent development of micro-cracks that might disqualify the specimen from further examination.

Next, powder layer of the NbC, TaC, TiC, VC or WC carbides with the average thickness of 0.05 mm bound with the inorganic binding agent was put down properly onto the degreased specimens. The siliceous liquid glass consisting of the Na₄SiO₄ orthosilicate and Na₂Si₂O₅ sodium disilicate was used as a binding agent in the form of the syrup like solution obtained under the increased pressure. Selected properties of powders are given in Table 2.

Rofin DL 020 high power diode laser (HPDL) was used for remelting and alloying with carbides the 55NiCrMoV7, 32CrMoV12-28, X40CrMoV5-1, and X38CrMoV5-3 steels; its technical specification is given in Table 3. The laser used is a high power unit, a versatile one, and used in materials engineering among others for cladding, welding, remelting, and surface enrichment. The laser system consists, among others, of the following modules: laser head, rotating work table, movable in the X-Y plane, protective gas nozzle, power supply and cooling

Table 1.
Chemical compositions of the investigated steels

Steel grade	Mass concentration of the elements, %								
	C	Mn	Si	Cr	W	Mo	V	P	S
55NiCrMoV7	0.55	0.75	0.25	1.1	-	0.50	0.10	0.025	0.019
32CrMoV12-28	0.308	0.37	0.25	2.95	-	2.70	0.535	0.020	0.020
X40CrMoV5-1	0.41	0.44	1.09	5.40	0.01	1.41	0.95	0.015	0.010
X38CrMoV5-3	0.372	0.43	0.42	4.95	-	2.72	0.42	0.022	0.022

Table 2.
Selected properties of carbide powders

Powder	Average grain size, μm	Melting point, $^{\circ}\text{C}$	Density g/cm^3	Hardness, HV
Niobium carbide	10	3500	7.6	2100
Tantalum carbide	10	3880	15.03	1725
Titanium carbide	3	3140	4.25	2800
Vanadium carbide	1.5	2830	5.36	2850
Tungsten carbide	5	2770	15.6	2600

Table 3.
Specification of the HPDL Roфин DL 020 diode laser

Laser radiation wavelength, nm	808 \pm 5
Laser beam output power (continuous wave), W	2300
Power range, W	100-2500
Laser beam focal length, mm	82 / 32
Laser beam spot dimensions, mm	1.8 \times 6.8
Power density range in the laser beam plane, kW/cm^2	0.8-36.5

systems, and the computer system controlling the laser operation and work table positioning. The rectangular or linear spot size is its significant advantage apart of its versatility, reliability, and small size. Remelting and alloying of surface layers were made using the powders shown in Table 2 in the power range from 1.2 to 2.3 kW. Dimensions of the laser beam focused on the material surface are 1.8 x 6.8 mm. The working focal length (measured from the protective glass in the head) is 92 mm. Remelting was carried out perpendicularly to the longer side of the focused beam with the multimode energy distribution, which makes it possible to obtain the wide run face.

It was found out in the preliminary investigations that the maximum feed rate at which the process is stable is 0.5 m/min. Further experiments were carried out at the constant remelting rate, changing the laser beam power in the 1.2-2.3 kW range during remelting and alloying the surface layer of the test pieces. It was revealed that the argon blow-in with the flow rate of 20 l/min through the \varnothing 12 mm circular nozzle oppositely directed in respect to the remelting direction provides full remelting zone protection. The test pieces were machined after remelting and alloying, to remove the non-remelted layer of the used carbides.

3. Investigation methodology

Test pieces from the 55NiCrMoV7, 32CrMoV12-28, X40CrMoV5-1, and X38CrMoV5-3 steels subjected to the standard

heat treatment and laser alloyed were cut in the plane perpendicular to the remelting direction on the Struers Discotom-2 device. The cutting disk was water cooled. The prepared test pieces were hot-mounted in the thermosetting resin within 12 min, out of which 7 min were for heating the resin up and the specimens were cooled for 5 min. The microsections were prepared by grinding on abrasive papers and buffing on diamond abrasive compounds using Struers devices, with subsequent etching. Etching time was selected experimentally for each investigated material's surface layer form. Metallographic examinations were made on the Leica MEF4A light microscope equipped with the Leica-Qwin computer image analysis system at magnifications of 100-1000 \times and on the Opton DSM-940 scanning elektron microscope. The Leica-Qwin computer image analysis system was used for thickness examination of the particular zones of the surface layer and for measurement of areas of grains. The saved examination results of the average grain size and dendrite lengths in the particular zones were analysed statistically.

Diffraction and chemical composition examinations in micro-areas and of the thin foil structures were made on the JEOL 3010 HRTM transmission electron microscope at the accelerating voltage of 300 kV, equipped with the Oxford EDS LINK ISIS X-ray energy dispersive spectrometer and on the Zeiss SUPRA 25 electron microscope at the accelerating voltage of 120 kV. Thin foils were made from lamellae diced on the electro-discharge machine from the test pieces for the structural examinations, from which disks with 3.2 mm O.D. were cut out, next mechanically thinned and ion polished in the electrolyte on the Struers

TENUPOL-2 electrolytical polishing device and on the Gatan 691 ion polishing device. The diffraction patterns from the transmission electron microscope were solved using the „Eldyf” computer program. Analysis of the crystallographic relationships occurring between the phases identified in the diffraction patterns from thin foils was made using the stereographic projections.

The X-ray qualitative and quantitative micro-analysis and analysis of the surface distribution of the alloying elements in the test pieces of the investigated steel, subjected to the standard heat treatment and remelted and alloyed, were made on the Opton DSM-940 scanning electron microscope with the Oxford EDS LINK ISIS X-ray energy dispersive spectrometer at the accelerating voltage of 120 kV and on the JEOL JCSA 733 X-ray micro-analyser.

Hardness tests were made with Rockwell method in C scale on specimens subjected to the standard heat treatment and remelted and alloyed using the high power diode laser at various parameters, making 10 measurements for each condition and calculating their average value. Test results were analysed statistically. Hardness was measured on the ground and buffed front surfaces of specimens.

Examinations of micro-hardness changes across the laser runs versus distance from the surface were carried out on the Shimadzu DUH 202 ultra-microhardness tester. The tests were carried out at 0.1 N load, making the necessary number of indents on the section of each examined specimen, correspondingly to the structural changes depth in the material surface layer. The microhardness tests were made along the lines perpendicular to specimens' surfaces, along the run face axis.

Abrasion wear resistance tests of the surface layers in the metal-ceramic material arrangement were carried out on a device developed in the Department of Welding of the Silesian University of Technology according to the ASTM standard. The surface layer obtained consisted of four adjacent welding sequences. Two test pieces of each type of the investigated gradient surface coatings were examined according to the requirements of the standard. The ceramic material - quartz sand with the granularity of 212-300 μm - was delivered by the nozzle with the flow rate of about 350 g/min during the test. The nozzle was between the examined test piece and the rubber circle with the diameter of 229 mm. The test piece was loaded with the constant force of 130 N and was pressed down to the rotating rubber wheel. The test pieces before and after the grindability examinations were weighed on the analytical balance with the accuracy of 0.0001g to check the mass loss, depending on the used particles and laser power. The 55NiCrMoV7, 32CrMoV12-28, X40CrMoV5-1, and X38CrMoV5-3 conventionally heat treated steels were used as reference materials.

Thermal fatigue tests for the 55NiCrMoV7, 32CrMoV12-28, X40CrMoV5-1, and X38CrMoV5-3 steels were carried out on a stand of the Institute of Engineering Materials and Biomaterials. The test pieces were induction heated by a heating coil encompassing half of the test piece perimeter powered by the ELCAL REL – 15 induction generator with the current frequency of 400 kHz and maximum power of 15 kW. The test piece rotating at about 25 rpm was immersed in the overflow tank at a depth of ca. 20 mm, cooling with the running water. Experiments were carried out for each type of the test pieces alloyed with the hard particles at different laser power values.

The maximum temperature of the surface of test pieces did not exceed $580\text{ }^{\circ}\text{C} \pm 1\%$. It was measured at the output of the test piece from the heating coil using the MINOLTA LAND Cyclops 152 optical pyrometer and it was regulated using the generator. Temperature changes in the test pieces surface layer during the thermal cycle were registered on the x-y logger connected with the thermocouple welded with the standard sample at 0.2 mm depth under the heated surface. Fragments were cut out for metallographic examinations from the test pieces subjected to 5000 thermal cycles; the examinations were carried out in the Leica MEF4A light microscope using the Leica Qwin computer image analysis system. Examinations were made on the Opton – DSM 940 scanning microscope of surfaces of the test pieces after thermal fatigue. The average cracks depth, the maximum cracks depth (calculated as an average from 3 deepest cracks) and the number of cracks per 1 mm of the test piece perimeter were assumed as criteria specifying the thermal fatigue resistance of the investigated steels.

Temperature measurement during remelting was carried out using the non-contact digital IMPAC IS 140 pyrometer designed for measurement of temperature of metals and ceramics. The pyrometer is connected through the RS232 port to the PC computer on which the InfraWin PC application is installed making it possible to log the temperature change cycles.

The artificial neural networks were used to determine the effect of the technological conditions of laser alloying on hardness of the hot work tool steels. Statistica Neural Networks program environment was used for calculations. Data set necessary to develop the network model for determining hardness and micro-hardness of the hot work tool steel after laser treatment of its surface layer by alloying with carbides was collected based on the experimental data acquired from the literature and also obtained from own research. Input data are classified according to:

- mass concentration of the elements,
- power of the laser used for surface treatment,
- type of the alloying material used,
- distance from the test piece surface (in micro-hardness tests),
- HRC hardness,
- HV micro-hardness.

Selection of the network types for the particular tasks was made from among:

- MLP multilayer perceptron,
- linear network,
- RBF radial base functions network,
- GRNN generalised regression neural network.

The following training methods were considered for selection of the network training:

- error backpropagation,
- conjugate gradients,
- quasi-Newton,
- Levenberg–Marquardt,
- fast propagation.

The artificial neural networks were used to determine relationships between the laser power, chemical composition of steel, alloying material type, and mass loss during the abrasion wear test. Input data included the alloying material type, laser power used for alloying, and the chemical composition of the steel. Data set consisting of 285 cases was randomly split into three subsets: training set (143) – used for modification of weights in the network training process, validation set (71) – used for the

network quality evaluation carried out in the training process, and the testing set used for assessment of the model efficiency after completing the neural network training procedure. Experimental data acquired for the 32CrMoV12-28, X40CrMoV5-1, and X38CrMoV5-3 steels subjected to laser alloying were used to develop the artificial neural network for determining the abrasion wear resistance of the hot work tool steels. The MLP (multi-layer perceptron) unidirectional network was used for development of the artificial neural network model for determining the abrasion wear resistance of the hot work tool steel alloyed with the NbC, TaC, TiC, VC, and WC carbides with the high power diode laser. The error backpropagation- and conjugate gradients algorithms were used for training the neural network. The training process was completed after 50 training epochs for the backpropagation algorithm and after 342 training epochs for the conjugate gradients algorithm. The number of neurons in the input layer was determined (14), representing the mass concentrations of elements in steel, alloying material type, and laser power used for alloying.

The obtained neural network models were numerically verified using data, that were not used in their development. Hardness and micro-hardness values calculated for the verification set were compared with the experimental results obtained for the X38CrMoV5-3 steel.

The following quantities were used as the main quality coefficients of the model developed using the neural network:

- average network prediction error,
- standard deviation of the network prediction error,
- quotient of standard deviations,
- Pearson's R correlation coefficient,
- histogram of the network prediction error,
- error dispersion plot.

The average network prediction error was calculated using the formula:

$$E_j = \frac{1}{n} \sum_{i=1}^n (|X_{zi} - X_{oi}|) \quad (1)$$

where:

E_j – error for the j-th property,

n – number of data in the training set,

X_{zi} – i-th measured value,

X_{oi} – i-th calculated value,

Standard deviation of the network prediction error was determined according to the formula:

$$s = \sqrt{\frac{n \sum_{i=1}^n E_i^2 - (\sum_{i=1}^n E_i)^2}{n(n-1)}} \quad (2)$$

Quotient of standard deviations for errors and data was assumed as an essential quality coefficient for the model developed using the neural network. Correctness of the model accepted by the network may be considered only when predictions presented by the network are encumbered with a smaller error than a simple assessment of the unknown output value. The simplest way to assess the output value is to assume the average value of the output values for the training set and presenting it as a prediction for data that were not presented during the training process. In this case the average error is equal

to the standard deviation for the output value in the training set, whereas the quotient of standard deviations assumes value of one. The smaller is the network prediction error is the smaller values assumes the quotient of standard deviations reaching zero for the "ideal" prediction.

The standard R^2 Pearson's correlation coefficient for the expected value and for the calculated value at the output of the neural network was calculated using the formula:

$$R^2 = \frac{n \left(\sum_{i=1}^n X_{zi} X_{oi} \right) - \left(\sum_{i=1}^n X_{zi} \right) \left(\sum_{i=1}^n X_{oi} \right)}{\sqrt{\left(n \sum_{i=1}^n X_{zi}^2 - \left(\sum_{i=1}^n X_{zi} \right)^2 \right) \left(n \sum_{i=1}^n X_{oi}^2 - \left(\sum_{i=1}^n X_{oi} \right)^2 \right)}} \quad (3)$$

Representation of the relations between the output and real values was worked out as error dispersion plots presenting in two dimensions cases belonging to various classes, which are determined by the real variable from the data set and the nominal variable – predicted by the network. Network response surface plots were used for visualisation of the neural network behaviour, which convey an idea of the way the network outputs change depending on two selected input variables. Network prediction error size distribution is presented in the form of bar charts.

Predicted hardness for the verification set is presented in line plots depending on the laser power used. Micro-hardness prediction for the verification set is presented in line plots as a function of distance from the steel surface of the investigated test piece. The plots were made for every alloying material and laser beam power.

4. Discussion of the experimental results

Presented investigation results pertain to fabrication of the gradient surface layers of tools in service at elevated temperature and to supplementing the traditional heat treatment used to date for this type of tool materials. Laser alloying of the investigated steels with particles of hard phases makes behaviour prediction of this material in service complicated. Superposition of stress fields interaction, dislocation movements, presence of micro-cracks, results in development of a very complex system, much more complicated than in case of the hot work tool steels unalloyed with the hard phases powders. Improved abrasion wear resistance, mechanical-, and tribological properties, and also very high resistance to thermal fatigue displayed by these materials, can be obtained in particular by alloying with the NbC, TaC, TiC, VC, and WC carbides particles. Not only the right selection of the hard phases powder used for alloying but also its distribution and volume portion in the matrix, modelled later by various technological operations decides the further service properties of the completed product.

The main research goal is modelling the gradient structure leading to attaining properties of the surface layer impossible to obtain by the conventional heat treatment. Therefore, the practical goal of such treatment is obtaining the supersaturated fine-crystalline layers, characteristic of a significant chemical diversity and metallurgical purity, which leads to gradient change of hardness

and service properties of the surface layer as a consequence of the fast crystallization due to solidification of metal.

It was revealed, basing on the metallographic examinations, that the structure of the material solidifying after laser alloying is characteristic of occurrences of areas with the gradient diversified morphology connected with crystallisation of the steel. Material surface is heated quickly to the temperature of 3420°C (Fig.1) when the laser beam acts on it and the strong circulation of the molten material takes place, followed by rapid solidification when the laser beam has passed. This phenomenon is the reason for the super-fast phase transformations affecting the structural mechanism of forming the surface layers subjected to laser treatment. Occurrences of the remelted- and heat affected zones have been confirmed in the surface layers of the investigated steels, whose thickness depend on the employed laser treatment parameters and type of the hard phases particles (Fig. 2-5). The subsequent growth of the remelting zone and of the heat affected zone is also connected with the laser radiation absorption effect by the surface of test pieces covered with carbides and is proportional to the employed laser power. The biggest, from among all investigated steels, remelted zone thickness of 1.31 mm was revealed in case of the X40CrMoV5-1 steel alloyed with the TaC carbide with the laser beam power of 2.3 kW (Fig. 2-5), and the smallest remelted zone thickness of 0.29 mm is characteristic of the 55NiCrMoV7 steel alloyed with the niobium carbide with the laser beam power of 1.2 kW.

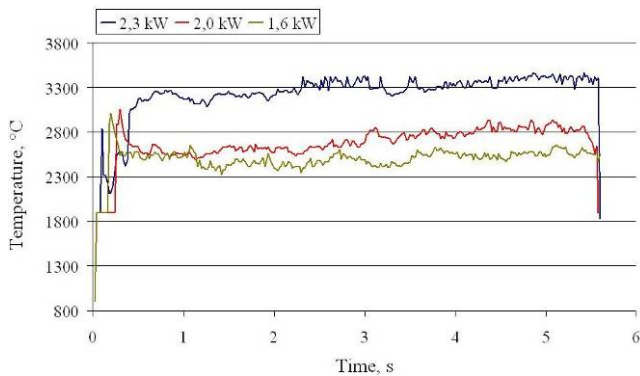


Fig. 1. Temperature changes as a time function during laser remelting of the surface layer of X38CrMoV5-3 steel with laser power of 1,6 to 2,3 kW

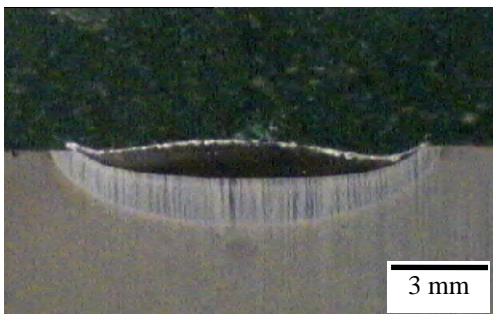


Fig. 2. Surface layer of the 32CrMoV12-28 steel alloyed with TaC powder with parameters: alloying rate – 0.5 m/min, laser power 2.3 kW

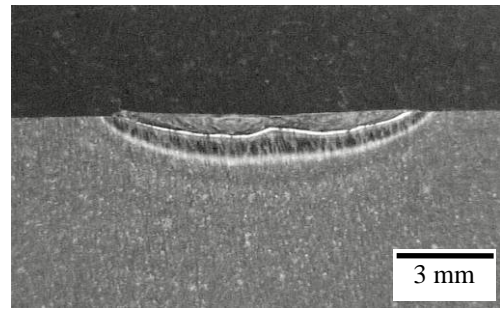


Fig. 3. Surface layer of the X40CrMoV5-1 steel alloyed with WC powder with parameters: alloying rate – 0.5 m/min, laser power 2.3 kW



Fig. 4. Surface layer of the X40CrMoV5-1 steel alloyed with NbC powder, laser power 2.0 kW

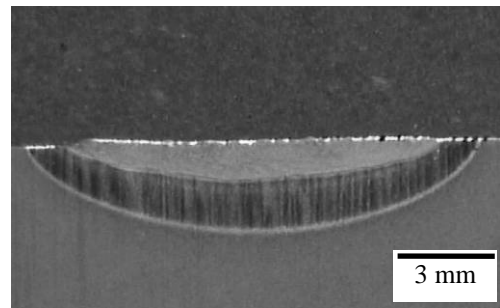


Fig. 5. Surface layer of the X38CrMoV5-3 steel alloyed with TaC powder, laser power 2.0 kW

During alloying with carbide powders: NbC, TaC, TiC, VC, and WC, whose melting temperature is much higher than the melting points of the investigated steels, penetration occurs of the undissolved carbide powder grains into the molten steel substrate (Figs. 6, 7). Carbides remain undissolved in certain cases, forming conglomerates (Figs. 8, 9). Increasing the laser power results in decrease of the portion of the undissolved carbides dispersively hardening the remelted matrix of the steel surface layer. Fast crystallization leads to differentiation of structure in the cross section of the remelted zone for all investigated steel grades (Figs. 10, 11). The characteristic repeated crystal growth direction change is observed for these areas. Small dendrites occur in the area at the boundary between the solid and liquid phases, whose main axes are oriented according to the heat transfer directions (Fig. 11). The significantly smaller sizes of crystals in this zone, compared to the central remelting area (Fig. 11), are

connected with initiating the solidification process on the undissolved carbides and partly melted grains of the native material. Consecutive stages of crystals growth (cellular-dendritic and dendritic) are closely connected with retaining the privileged orientation - crystals growth direction corresponds with the direction of the biggest temperature gradient, assuming that the entire specimen's material volume receives remelting process originated heat. Structure of fine equiaxial crystals with the carbide lattice develops in the central zone of the fused area where heat abstraction takes place in all directions (Figs. 12, 13). Mixing of materials proceeds according to various mechanisms, depending on the employed laser treatment parameters. Capillary lines are not connected and the remelting structure is relatively homogeneous at low energy values of the laser impact on the material (Figs. 14, 15). At the low laser beam power the tantalum or niobium carbides introduced into the surface layer during alloying dissolve partially originating clusters of carbides (Figs. 8, 9); whereas, laser power increase causes their partial dissolution in the investigated steel matrix especially at grain boundaries. Similarly, after the laser alloying of steel with the TiC, VC, and WC these carbides dissolve partially originating conglomerates of carbides (Figs. 16, 17), and the laser power increase causes their partial melting, the local concentrations of niobium, tantalum, vanadium, titanium, and tungsten exceed the equilibrium concentrations in the alloyed surface layer. In case of alloying with the WC carbide presence of tungsten carbide was revealed in the surface layer developed by alloying (Figs. 18, 19) and in the interdendritic spaces enriched in tungsten coming from the dissolved particles of the alloying material.

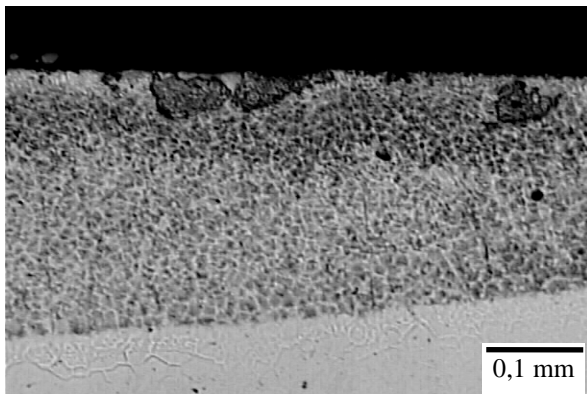


Fig. 6. Boundary of the remelted surface layer of the X38CrMoV5-3 steel alloyed with NbC powder, laser power 1.2 kW

In all investigated steel grades grouping of the alloying elements was confirmed at dendrite boundaries in the area of the superfine eutectics occurring in the remelted zone due to fluctuation of the chemical composition, especially at the remelting bottom (Fig. 20). The capillary lines swirl occurs along with the laser power increase which begin to link and the occurring carbides' conglomerates form the characteristic swirls (Figs. 20, 21). The remelting bottom is flat in this case, however slight waviness appears often on surface (Figs. 2, 4, 21). Employment of the maximum laser power results in obtaining the maximum remelting thickness of the surface layer; however, the remelting bottom gets wavy because of the strong liquid motions

(Fig. 3). Carbides introduced into the steel are present in the remelted zone only (Fig. 22); however, their concentration grows at the dendrites boundaries (Fig. 23).

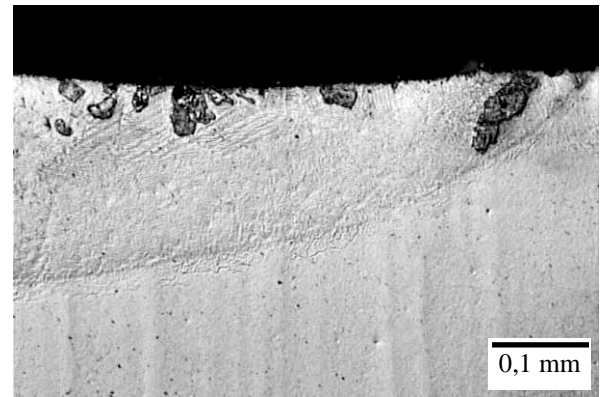


Fig. 7. Surface layer edge of the X38CrMoV5-3 steel alloyed with TaC powder, laser power 1.6 kW

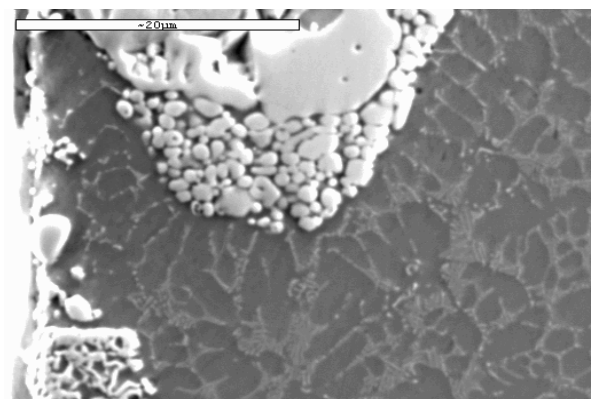


Fig. 8. Alloying material in the surface layer of the X40CrMoV5-1 steel after laser alloying with TaC powder, laser power 1.2 kW

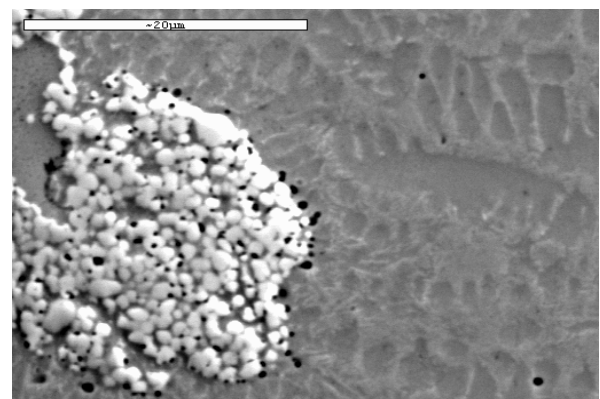


Fig. 9. Alloying material in the surface layer of the X40CrMoV5-1 steel after laser alloying with NbC powder, laser power 1.6 kW

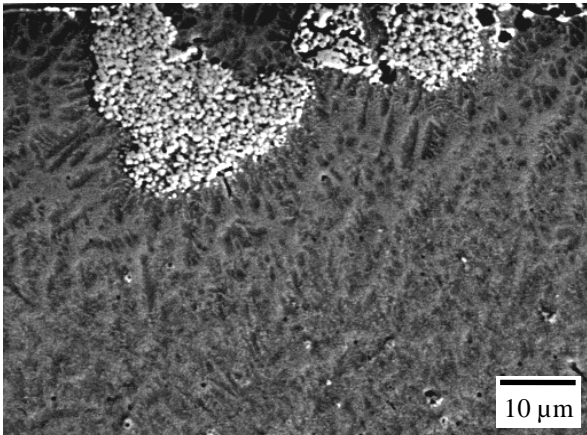


Fig. 10. Alloying material in the surface layer of the X38CrMoV5-3 steel after alloying with NbC powder, laser power 1.2 kW

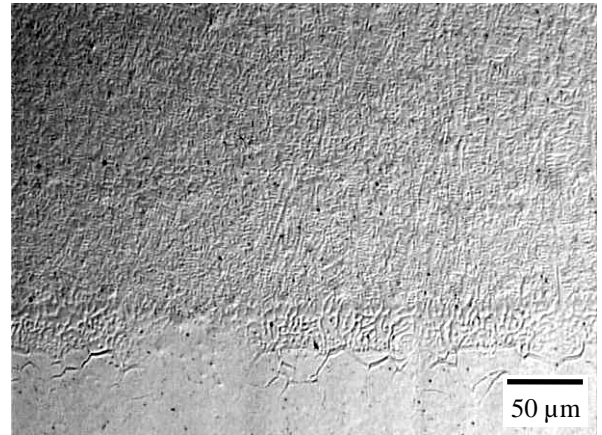


Fig. 13. Boundary of the alloying layer of the X38CrMoV5-3 steel after alloying with TaC powder, laser power – 1.6 kW

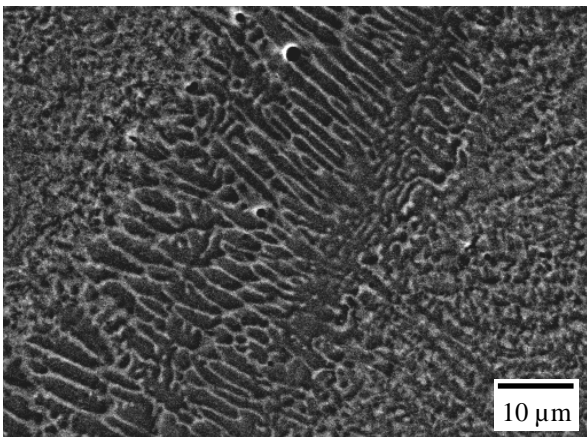


Fig. 11. Surface layer of the X38CrMoV5-3 steel after alloying with NbC powder, laser power 2.3 kW

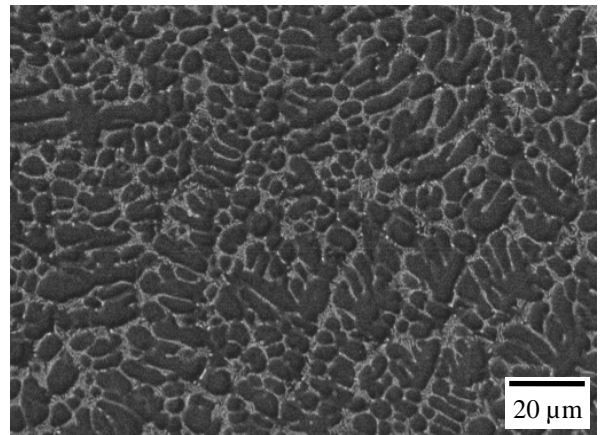


Fig. 14. Surface layer of the 32CrMoV12-28 steel after alloying with TaC powder, laser power– 1.6 kW

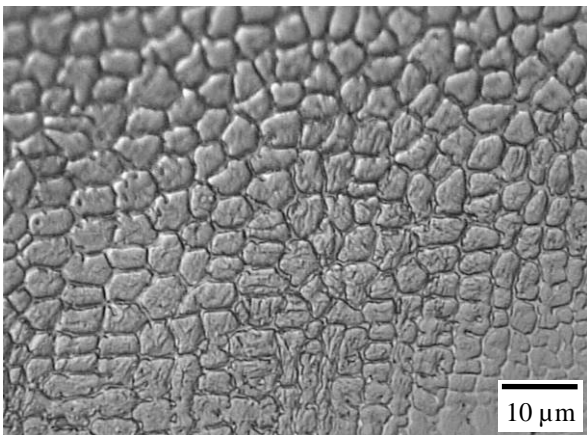


Fig. 12. Surface area of the surface layer of the X40CrMoV5-1 steel after alloying with WC powder, laser power – 1.6 kW

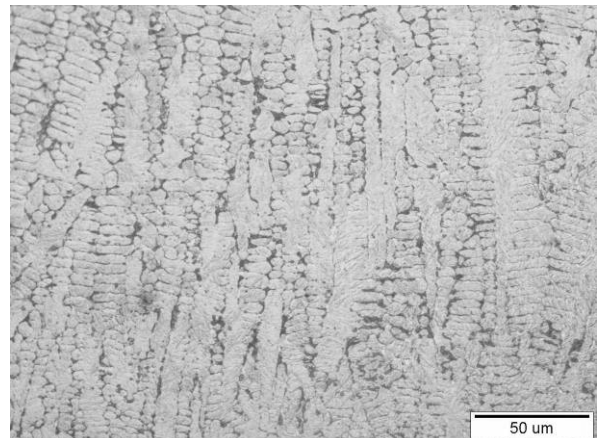


Fig. 15. Surface layer of the 55NiCrMoV7 steel after alloying with NbC powder, laser power– 2.3 kW

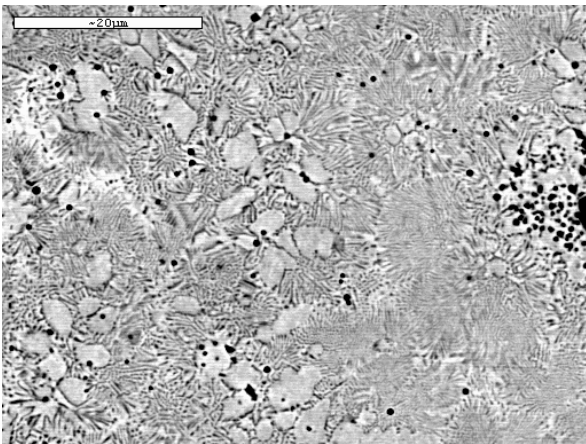


Fig. 16. Surface layer of the steel X40CrMoV5-1 after alloying with VC powder, laser power 1.6 kW

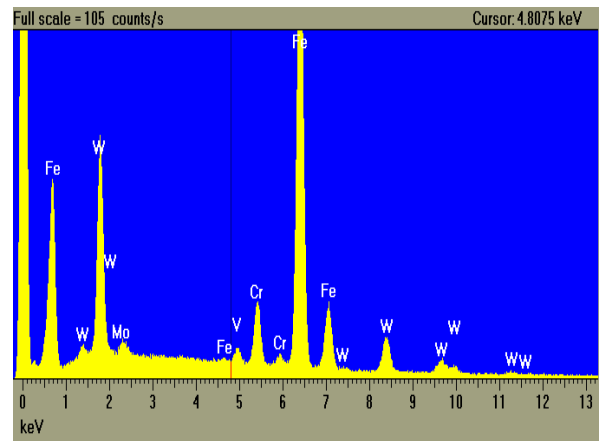


Fig. 19. EDS point-wise analysis of the X40CrMoV5-1 steel sample after laser alloying with WC powder, laser power 1.2 kW

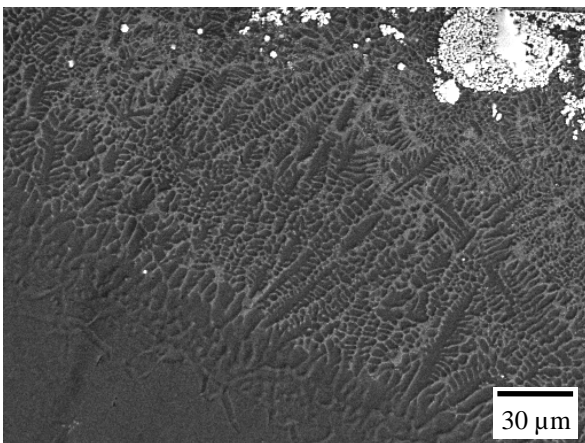


Fig. 17. Boundary of the remelted zone in the surface layer of the X38CrMoV5-3 steel after laser alloying with TiC powder, laser power 2.0 kW

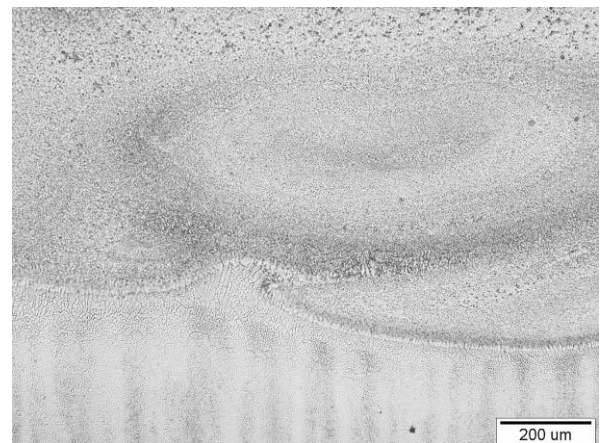


Fig. 20. Boundary of the remelted zone in the surface layer of the X40CrMoV5-1 steel after laser alloying with TiC powder, laser power 2.3 kW

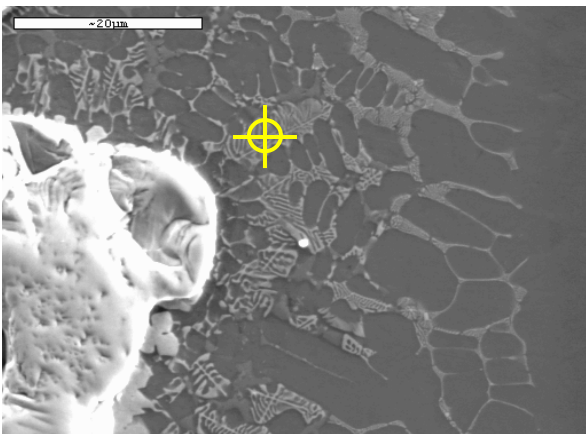


Fig. 18. Alloying material and small eutectic in the surface layer of the X40CrMoV5-1 steel after laser alloying with WC carbide, laser power 1.2 kW

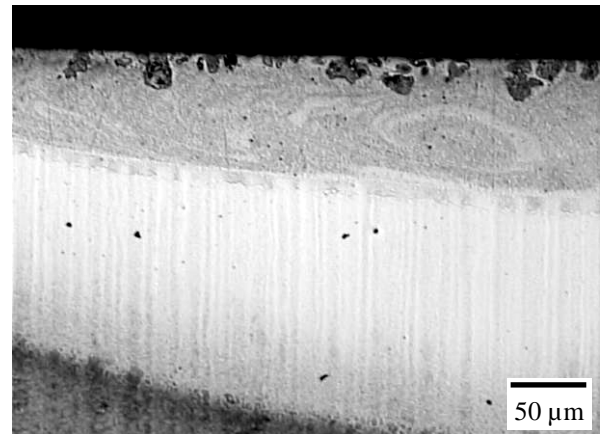


Fig. 21. Edge of the alloyed surface layer of the X38CrMoV5-3 steel after laser alloying with TaC powder, laser power 1.2 kW

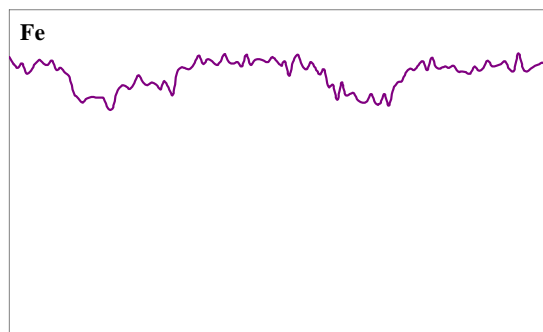
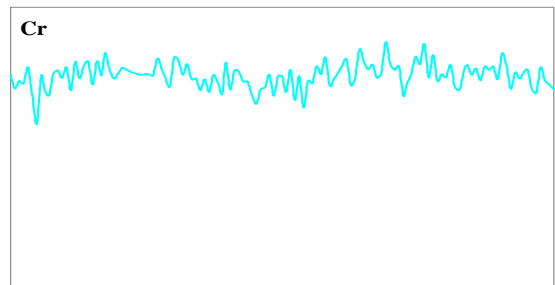
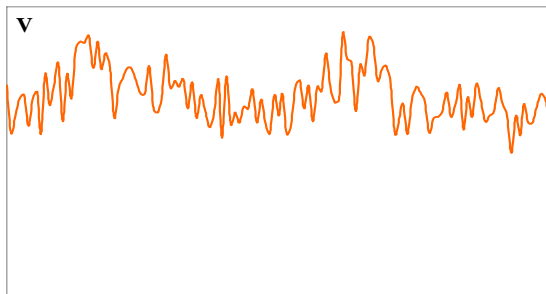
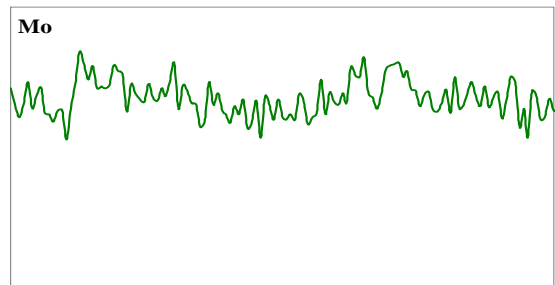
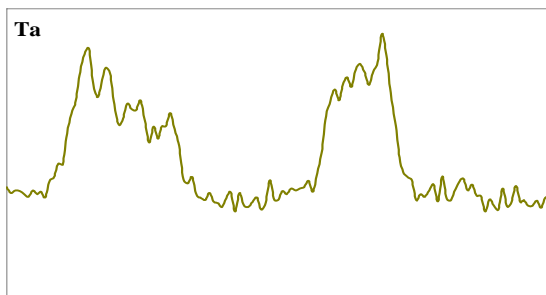
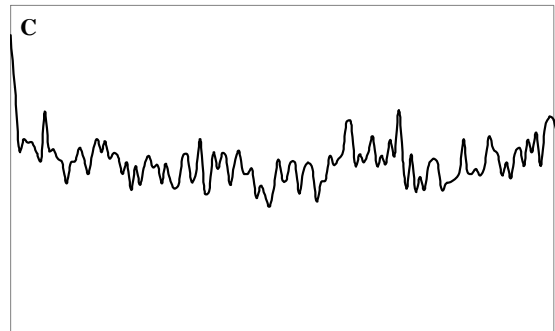
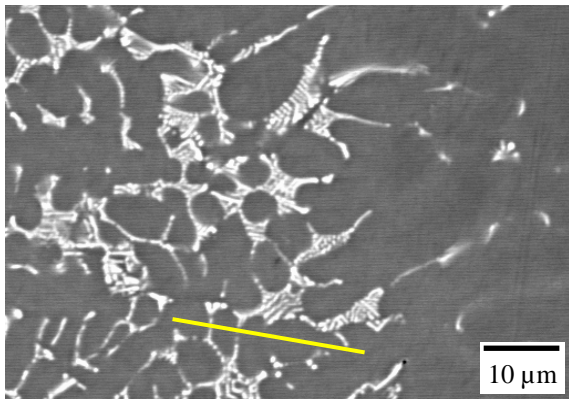


Fig. 22. Line-wise EDS analysis of the elements in the surface layer of the X40CrMoV5-1steel after laser alloying with TaC powder, laser power 1.2 kW

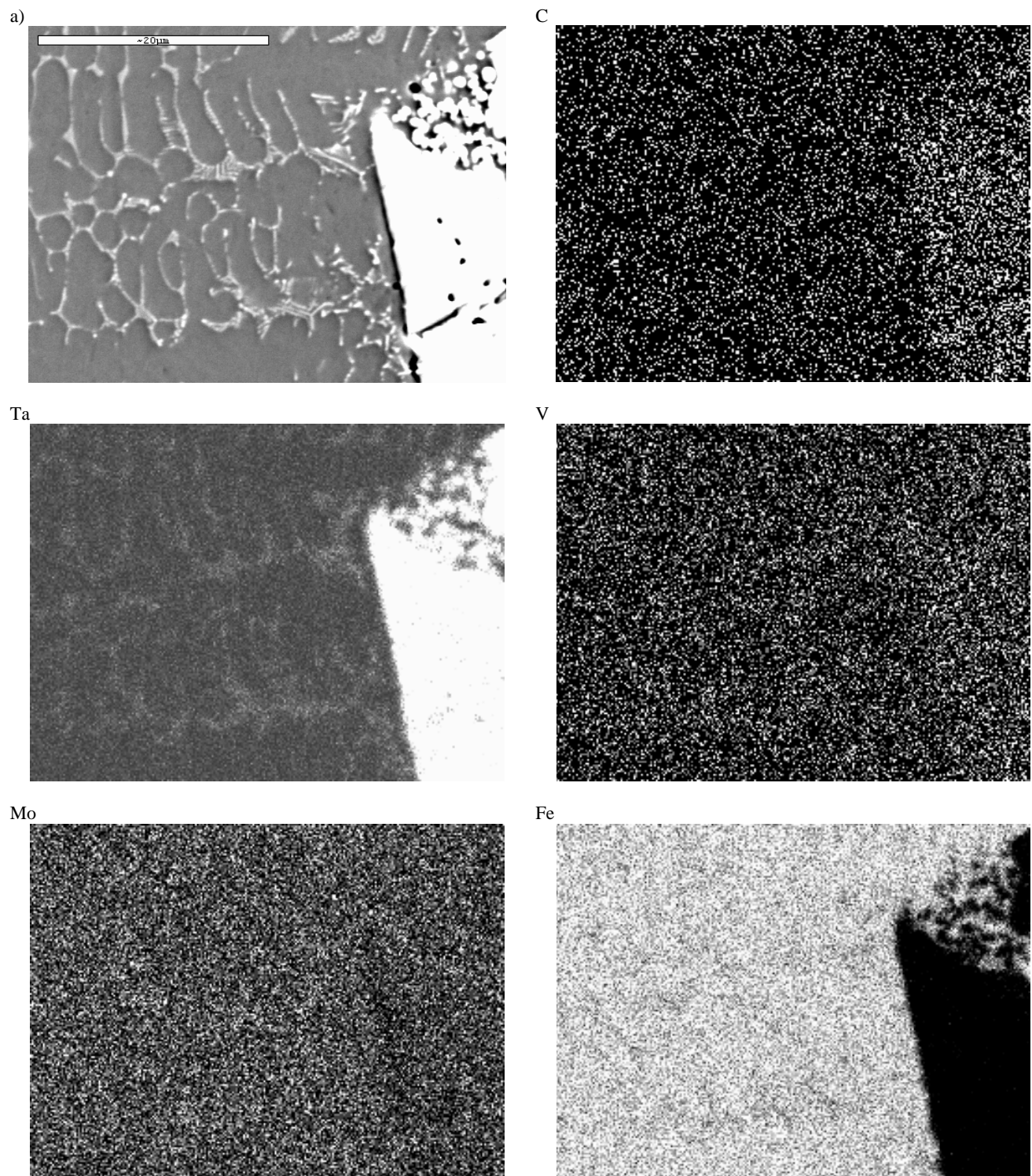


Fig. 23. Remelting zone in the surface layer of the X38CrMoV5-1 steel after alloying with NbC powder, laser power 2.3 kW, image obtained using secondary electrons (a) and mapping of elements distribution

Laser alloying with all of the above mentioned particles results in structure refinement in the entire investigated laser power range, which is presented with the X38CrMoV5-3 steel example (Fig. 24). Grains of varying sizes occur in the particular zones of the surface layer after laser alloying. The average grain sizes in the remelted zone of the investigated steels are for the particular particles in the ranges: niobium carbide from 6 to 28 μm^2 , tantalum carbide from 8 to 62 μm^2 , vanadium carbide from 10 to 12 μm^2 , titanium carbide from 20 to 43 μm^2 , tungsten carbide from 22 to 27 μm^2 . However, in the conventionally heat treated steel the average grain size is 248 to 312 μm^2 ; therefore, it is 5-10 times bigger. Only at the crystallization front, between the fused and heat affected zones, the elongated and smaller grains occur, which are subjected to partial melting and re-crystallization during laser treatment.

Examinations of the thin foils of the X38CrMoV5-3 and 32CrMoV12-28 steels alloyed with the vanadium carbide confirm that the increased vanadium concentration in steel results in the significant surface layer structure changes.

The discontinuous VC type carbide lattice develops in these conditions at the grains boundaries (Figs. 25, 26). Sometimes they occur also inside of the grains as fine dispersive carbides. Lathe martensite with the high dislocation density as well as the retained austenite feature the matrix of the surface layer after alloying. However, examinations of thin foils made from the surface layer of the X40CrMoV5-1 hot work tool steel alloyed with the niobium-, vanadium-, tantalum- (Fig. 27), and titanium carbides (Fig. 28) revealed occurrences on grain boundaries of carbides used for alloying, e.g., of the NbC, VC, and TaC types. Lathe martensite with the high dislocation density features also the matrix of the surface layer after alloying. Lathes of this martensite are very fine, with the irregular shape and are twinned to a great extent. In the martensite of the surface layer of the alloyed steels there are also fine carbides of the M_3C or M_7C_3 types (Fig. 28), and in the steel alloyed with the vanadium carbide – precipitations of the M_4C_3 type carbides. These carbides are located at the martensite lathes boundaries and at the micro-twins boundaries.

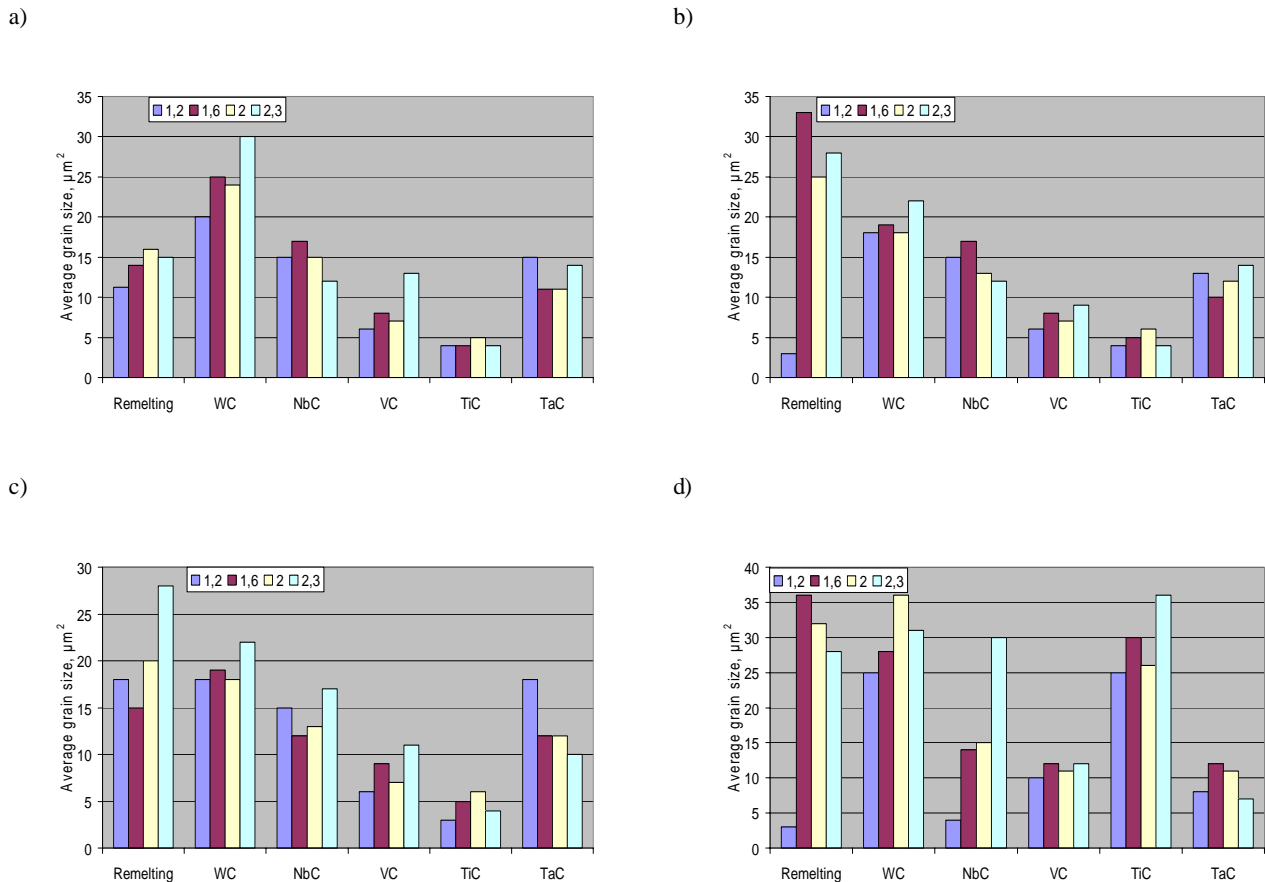


Fig. 24. Average grain size in the remelting area of the a) 55NiCrMoV7, b) 32CrMoV12-28, c) X40CrMoV5-1, d) X38CrMoV5-3 steels alloyed with carbides, laser power in the range of 1.2 to 2.3 kW

Laser treatment of surface layers results in the steel surface hardness increase of all investigated steels and this effect is achieved thanks to occurrences of phase transformations connected closely with the heat removal rate from the remelted zone. The factor controlling in great measure the cooling rate is thickness of the remelted layer, dependant on the absorbed radiation energy and the time period of the laser beam impact on the material. Only the laser power affects the energy delivered to the surface layer with the constant remelting rate. At the low power of the laser beam the remelting depth is small; therefore heat removal rate is the highest. High cooling rate causes occurrences of the super-fast phase transformations; therefore, the fine-grained martensite structure occurs in the material, responsible for hardness growth. The highest hardness of the steel surface layer reveals the X38CrMoV5-3 steel alloyed with the tantalum carbides, its maximum hardness growth to 67.4 HRC occurs at the laser beam power equal to 2.3 kW (Fig. 29). Hardness of the X40CrMoV5-1 steel surface layer alloyed with carbides grows compared to steel hardness attained after the conventional heat treatment, and its growth is proportional to laser beam power used

in the laser alloying process. The highest hardness for this steel of 62.6 HRC is characteristic of the surface layer alloyed with the VC vanadium carbide with the laser beam power of 2.0 kW and with the TaC tantalum carbide – 62.1 HRC with the laser beam power of 1.2 kW. One can state based on the hardness tests of the 32CrMoV12-28 steel subjected to laser alloying with the hard phases powders that for most of the powders the steel hardness was improved, compared to the steel subjected to the standard heat treatment only. The highest hardness growth is characteristic of the steel fused with the tantalum carbide and attains 66.3 HRC for 2.3 kW power, and the tungsten carbide – 59.4 HRC for 2.0 kW. As regards the 55NiCrMoV7 steel, it attains its highest hardness of 68.1 HRC after alloying with the WC carbide with the laser beam power of 2.3 kW, which is caused by a higher absorption of the laser radiation than in other cases by the hot work tool steel surface, and the resulting increase of the steel surface layer remelting. In case of the other carbides used for alloying of this steel, i.e.: tantalum-, titanium-, and niobium carbides hardness of the surface layer grows moderately compared to the steel after the standard heat treatment.

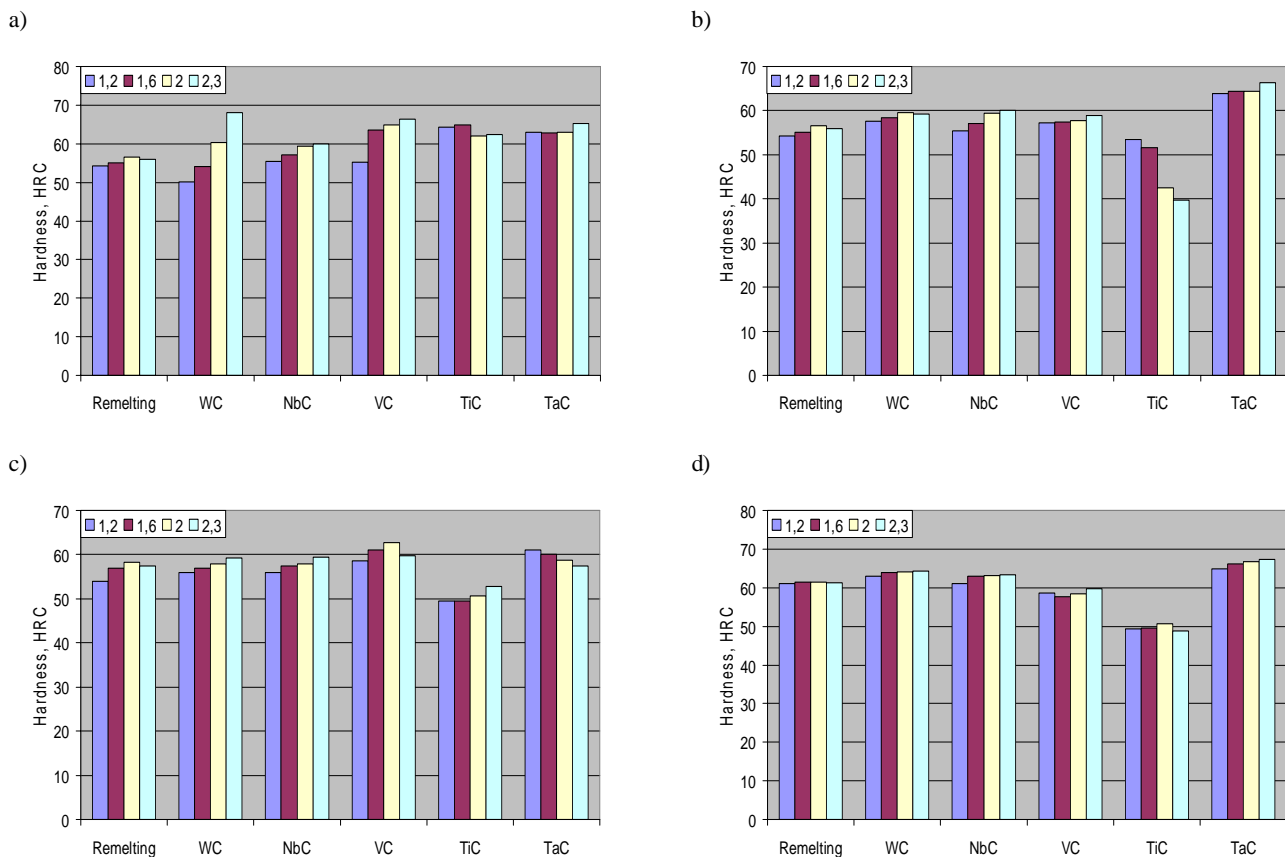


Fig. 29. Average hardness changes of the surface layer of the a) 55NiCrMoV7, b) 32CrMoV12-28, c) X40CrMoV5-1, d) X38CrMoV5-3 steels alloyed with carbides with variable laser power

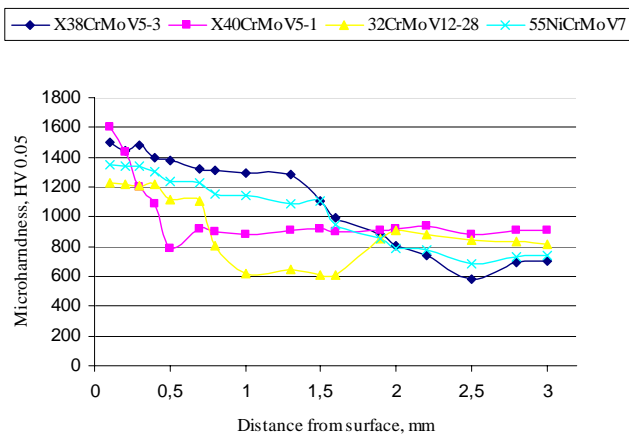


Fig. 30. Microhardness changes of the surface layer of the X38CrMoV5-3 steel after alloying with TaC powder, X40CrMoV5-1 steel after alloying with NbC powder, steel 32CrMoV12-28 after alloying with TaC powder, laser power 1.6 kW, steel 55NiCrMoV7-28 after alloying with TaC powder, laser power 1.6 kW

Figure 30 presents the flow of the gradient micro-hardness changes depending on the distance from the surface layer of the investigated steels. In case of all investigated steels alloyed with carbides the visible gradient micro-hardness growth occurs at the surface layer. The highest micro-hardness from all test pieces of steels subjected to laser treatment of 1412 HV_{0.01} is obtained at the laser power of 2.3 kW for the X38CrMoV5-3 steel alloyed with the tantalum carbide; whereas, the gradient layers obtained by alloying of the X40CrMoV5-1 steel are characteristic of the similar micro-hardness in the remelted area in the laser power range from 1.6 to 2.3 kW after alloying with the niobium carbide. The best effect in case of the 55NiCrMoV7 steel gives using the beam power of 2.3 kW. The highest micro-hardness in the fusion zone is characteristic of this steel alloyed with the tantalum carbide (1352 HV_{0.05}) and with the niobium carbide (1283 HV_{0.05}). However, the micro-hardness tests on the surface layer transverse section related to the distance from the surface of the examined test pieces give grounds to the statement that the gradient surface layers obtained after alloying the 32CrMoV12-28 steel with the TaC tantalum- and NbC niobium carbides are characteristic of the lowest micro-hardness of 1250 HV_{0.01} from among all investigated steels. One can notice the area in the micro-hardness measurement data plots with the clearly lowered hardness, about 500 - 600 HV_{0.01}. This decrease occurs for all examined test pieces alloyed with the hard phases powders. The hardness drop attests to development of the tempered material zone during laser treatment, heated to the temperature higher than the tempering temperature. Occurrences in the structure of the graded fused carbides and lattice of carbides at dendrites' boundaries, demonstrating hardness different from the substrate, feature the reason of the microhardness measurement results discrepancy for the remelted zone and the alloyed one on the transverse section of the laser paths versus distance from the surface.

Gradient hardness changes of the surface layers of the investigated steels, obtained by alloying with carbides using the high power diode laser, are usually accompanied by improvement of their tribological properties compared with the conventionally heat treated steel represented by their average mass loss (Fig. 31). The mass loss of the test pieces depends on the laser power for all investigated surface layer laser treatment methods. The minimum value of the average mass loss occurs in case of the X38CrMoV5-3 steel alloyed with the vanadium carbide. The highest average mass loss occurs in the surface layer of steel subjected to alloying with the tungsten carbide with the laser beam power of 1.2 kW. Also in case of alloying the X40CrMoV5-1 steel with the NbC or TaC carbides its abrasion wear resistance grows compared to the resistance of steel after the standard heat treatment. Improvement of the tribological properties is connected with the increase of steel hardness which is caused next with structure refinement. However, the abrasion wear resistance of this steel's surface alloyed with the tungsten carbide is lower than in case of using other carbide powders as alloying materials, and the cracks occurring in the surface layer reduce it significantly even more. In case of the 32CrMoV12-28 steel the lowest average mass loss occurs on surfaces alloyed with the titanium- and vanadium carbides. The extent of mass loss of the steel alloyed with the tungsten-, niobium, and tantalum carbide powders is comparable with the mass loss of the remelted steel. Also the abrasion wear resistance tests in the metal-metal setup, imitating the tool service in the industrial conditions (abrasive wear of dies, forging tools), confirm results of the previous research. In this setup also steel alloyed with the vanadium- and titanium carbides demonstrates the highest abrasion wear resistance. Investigations demonstrated that as a result of remelting the surface layer of the hot work alloy tool steels using the HPDL high power diode laser or its dispersive hardening by the innudated, or partially dissolved carbides, with the simultaneous enrichment of the surface layer with the alloying additives coming from the dissolving carbides hardness increase occurs and improvement of the tribological properties of the surface layer of the laser remelted or alloyed steel takes place, compared to the analogous properties of this steel after the conventional heat treatment.

Moreover, laser alloying of the 55NiCrMoV7, 32CrMoV12-28, X40CrMoV5-1, and X38CrMoV5-3 steels with the NbC, TaC, VC, WC, and TiC carbides results also in the thermal fatigue resistance improvement compared to the conventionally heat treated steel (Fig. 32). The reason for this phenomenon is the low number of cracks in the surface layer after alloying the investigated steel with the vanadium- and titanium carbides. In case of alloying the X38CrMoV5-3 steel with these carbides the fine cracks in the surface layer of the investigated steel occur after 5000 thermal cycles only, compared to the conventionally heat treated steel (Figs. 33, 34). However, in a steel alloyed with the TaC and WC carbides cracks and surface delamination of steel occur after 1000 thermal cycles only. The average depth of cracks developed during the thermal fatigue test was assumed to be the measure of the thermal fatigue resistance of the investigated X40CrMoV5-1 steel (Fig. 32). The average depth of cracks in case of the layer alloyed with the vanadium carbide is in the 0.02495 - 0.022 mm range, titanium carbide

0.024 - 0.016 mm, and with the tantalum carbide 0.024 - 0.018 mm. The maximum cracks depth values are in the 0.055 - 0.047 mm range for the vanadium carbide, 0.035 - 0.029 mm for the titanium carbide, and 0.045 - 0.011 mm for the tantalum carbide with the laser beam power values used of 1.2 - 2.3 kW. The investigations revealed that the highest thermal fatigue resistance is characteristic of the X40CrMoV5-1 steel alloyed with the titanium-, tantalum-, and vanadium carbides powders. The thermal fatigue resistance in case of alloying with the tantalum-, titanium-, or vanadium carbides grows compared to the resistance of the surface layers of steel treated in a conventional way. However, the lowest resistance in the test conditions demonstrate the surface layers obtained by alloying with the tungsten carbide in the entire laser power range. The type of the material used and technological conditions of laser treatment affect clearly improvement of the thermal fatigue resistance of the investigated 55NiCrMoV7 hot work tool steel. For this steel the lowest number of cracks is characteristic of the

test pieces alloyed with the TiC and VC carbides (Fig. 32). The smallest average depth of cracks in this test of the 32CrMoV12-28 steel is demonstrated, like for other investigated steels, by gradient layers alloyed with the tungsten carbide and titanium carbide powders (Figs. 35, 36). It was found out that the most advantageous power used for alloying with particles of both powders is the power of 2.3 kW. Proportional relationship is observed of increasing the thermal fatigue resistance from the laser power at alloying; at the low power (1.2 kW) this resistance is the lowest, and at the highest power (2.3 kW) this resistance grows. The most useful powders when thermal fatigue resistance growth of the laser alloyed 32CrMoV12-28 steel is considered are powders of the TiC titanium carbide and VC vanadium carbide; whereas, reduction of this resistance results from using powders of the tantalum- and niobium carbides, distinguished by originating the alloyed surface layers with very high hardness and abrasion wear resistance.

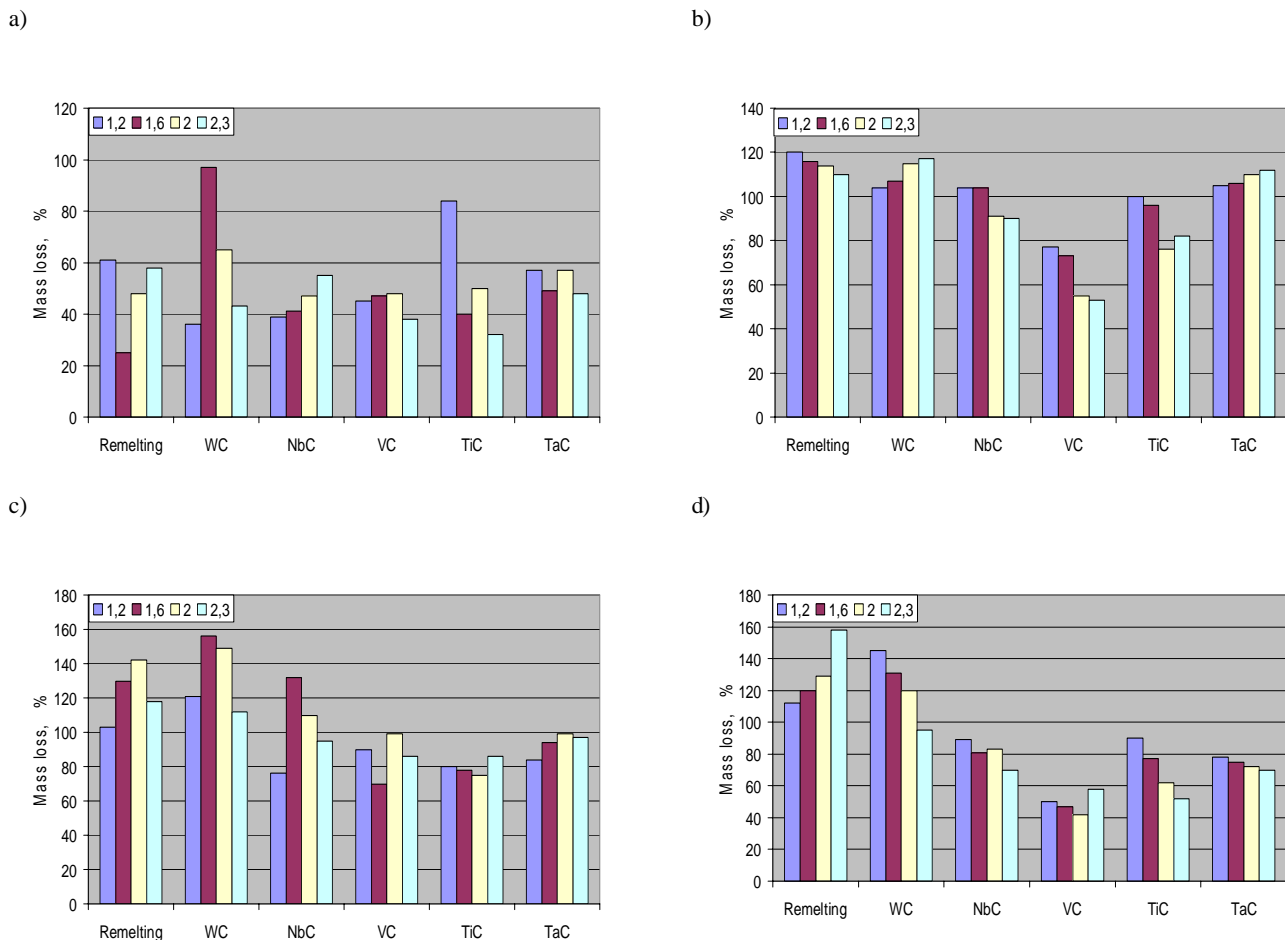


Fig. 31. Mass loss in comparison to the applied ceramic powder in the surface layer of the a) 55NiCrMoV7, b) 32CrMoV12-28, c) X40CrMoV5-1, d) X38CrMoV5-3 steels after alloying with NbC, TaC, VC, WC and TiC carbides with variable laser power

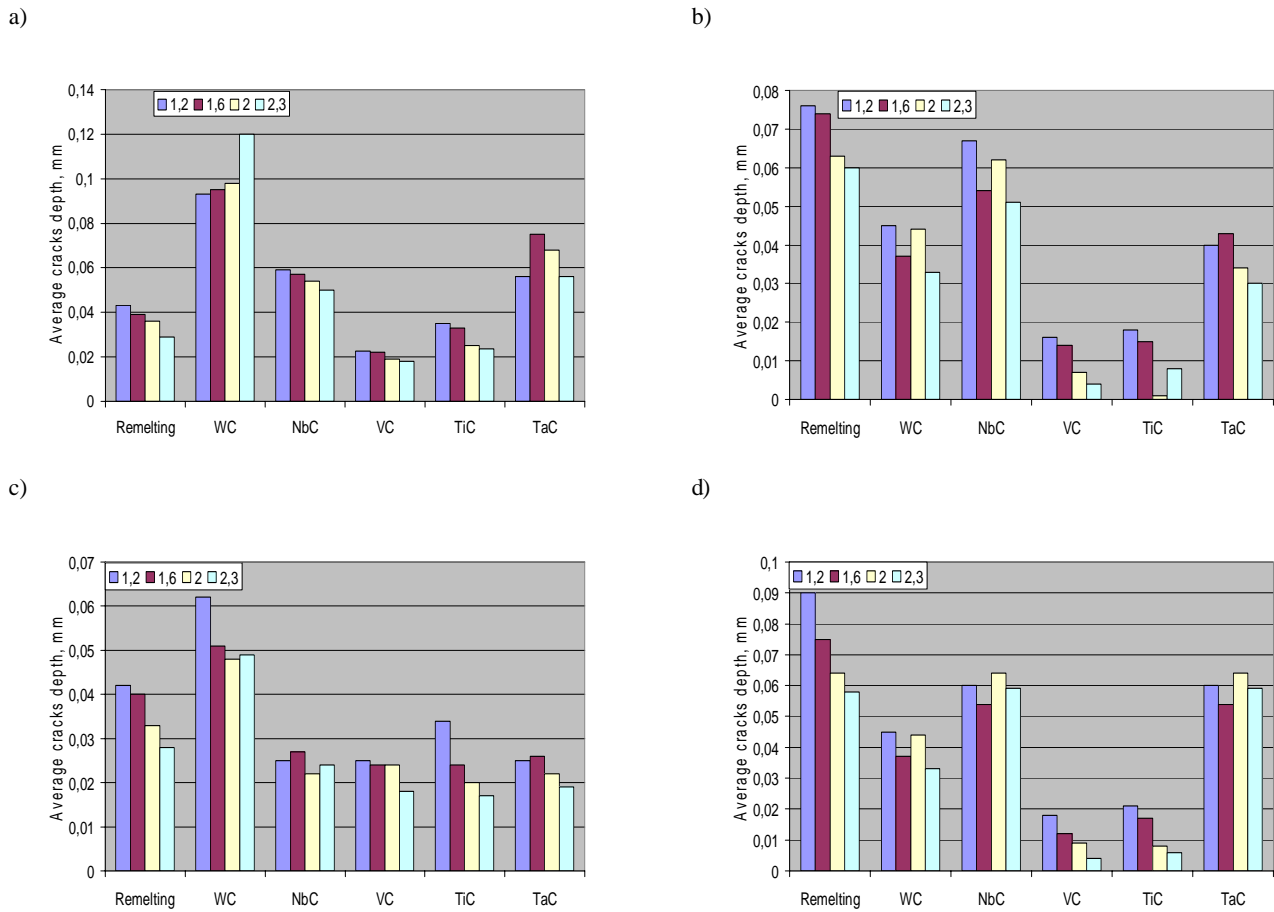


Fig. 32. Influence of heat treatment and laser power on the average cracks depth of the a) 55NiCrMoV7, b) 32CrMoV12-28, c) X40CrMoV5-1, d) X38CrMoV5-3 steels formed during the thermal fatigue test

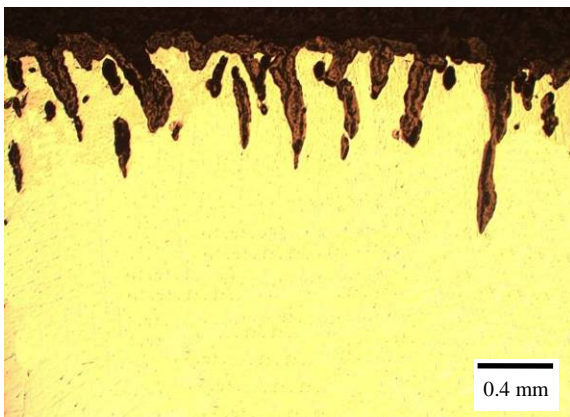


Fig. 33. Cracks on the cross-section of the heat treated X38CrMoV5-3 steel sample, formed during the thermal fatigue test

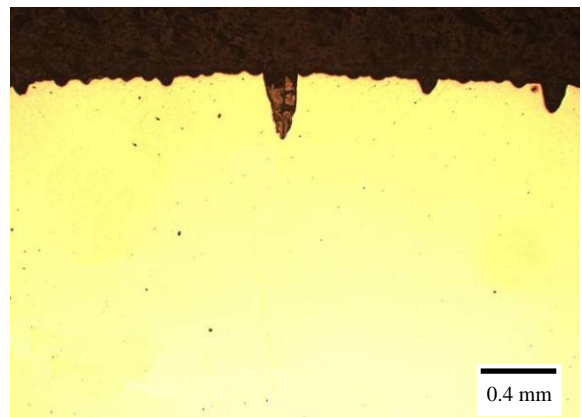


Fig. 34. Cracks on the cross-section of the TiC alloyed X38CrMoV5-3 steel sample, formed during the thermal fatigue test, laser power 1.6 kW

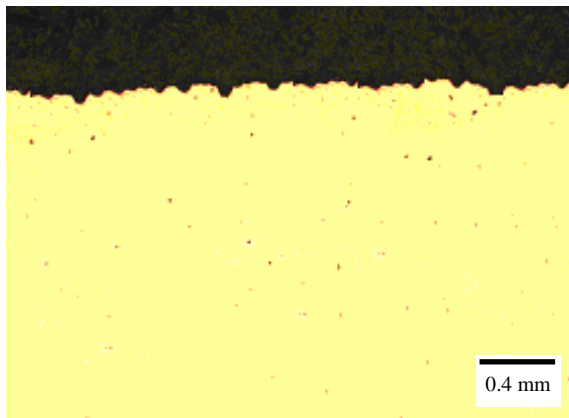


Fig. 35. Cracks on the cross-section of the VC alloyed 32CrMoV12-28 steel sample, formed during the thermal fatigue test, laser power 2.0 kW

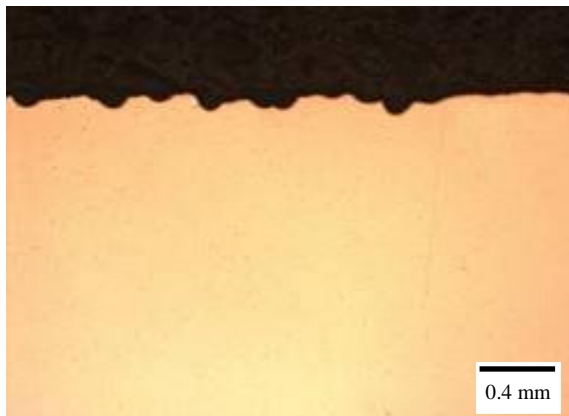


Fig. 36. rakes on the cross-section of the TiC alloyed 32CrMoV12-28 steel sample, formed during the thermal fatigue test, laser power 2.0 kW

Selection of the correct alloying elements and technological conditions of alloying ensuring obtaining the required gradient properties of the surface layer of the designed element enforces the use of the multicriterial optimisation which makes this procedure difficult and expensive. Therefore, the computer assisted system was developed for selection of the HPDL high power laser conditions connected with selection of the laser beam power and type of the carbide type alloying material. The task of the computer system is assistance in the alloying conditions selection aimed at obtaining the surface layer characteristic of the required mechanical properties. The artificial neural networks were used to achieve this goal.

The modelling methodology was developed within the framework of this project of the relationships between the chemical composition, alloying material type TiC, TaC, WC, VC, and NbC, and parameters of the laser surface treatment employing the artificial intelligence methods in the form of the neural networks. The developed model make analysis possible of

interaction of the alloying and remelting conditions on the main mechanical properties, i.e., hardness and micro-hardness of the hot work tool steels and make it possible to determine the mass loss during the abrasion wear test of the hot work alloy tool steel subjected to laser treatment.

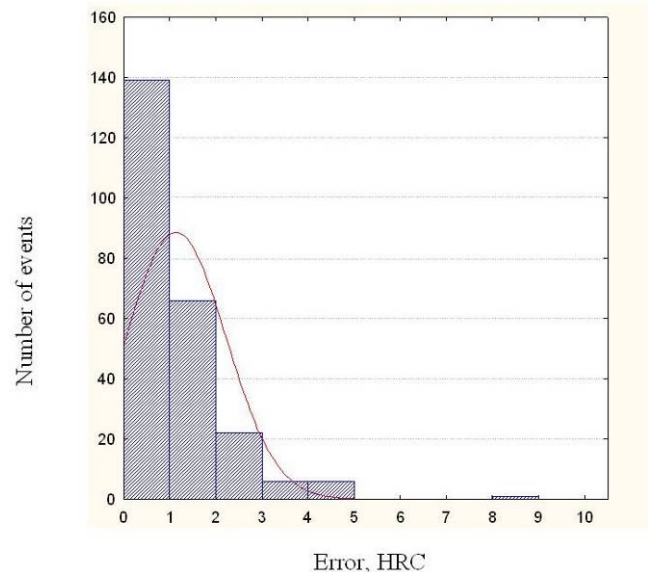


Fig. 37. Histogram of error for the hardness value calculated for a given testing data set using neural network

The unidirectional networks (MLP) with one hidden layer were used for development of the artificial neural network model for determining the hot work tool steel mechanical properties remelted or alloyed with the TiC, TaC, NbC, WC, and VC carbides with the HPDL high power diode laser. As a result of variables' optimization, the mass concentrations of elements were used at the input to the neural network, i.e., of C, Mn, Si, Cr, Mo, V, and Ni, and also the nominal variables representing the alloying material type TiC, TaC, NbC, VC, and WC in the laser surface treatment. Comparison of the consistence of the prediction results with the results of experimental research carried out for the X38CrMoV5-1 steel (Figs. 37, 38) show that the developed network models are functioning properly. Results of the comparative analysis give grounds for statement that the developed neural network model makes hardness prediction possible of the hot work tool steel after laser remelting or alloying with the average error of 1.8%, in case of the model for micro-hardness prediction with the average error of 6.6%. The developed network models make it possible to determine relationship between the laser beam power and mass concentrations of elements with the surface layer hardness (Fig. 39) and also to determine the relationship between the micro-hardness of the surface layer as a function of the distance from the surface of the hot work tool steel remelted or alloyed with the TiC, TaC, WC, VC, and NbC carbides and the laser beam power.

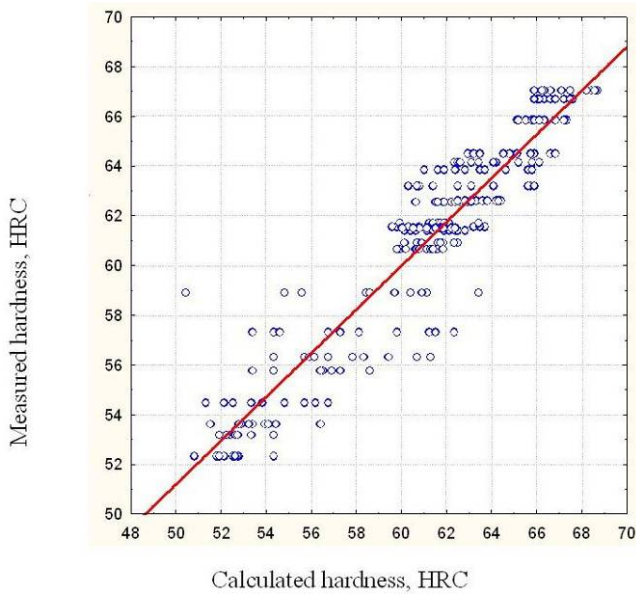


Fig. 38. Comparison of a measured HRC hardness and values calculated using neural network model for the test model

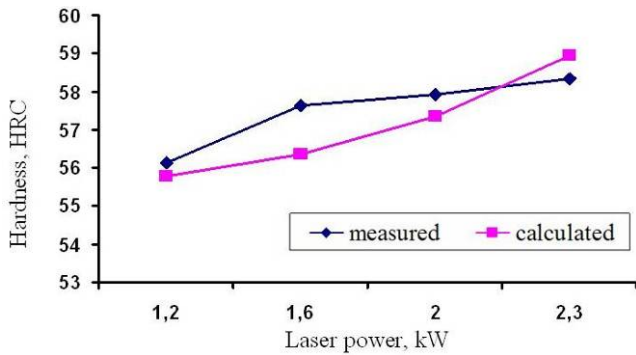


Fig. 39. Comparison of the measured and calculated hardness for the X38CrMoV5-3 steel alloyed using VC powder

The next modelled artificial neural network makes it possible to develop a model for the abrasion wear assessment of the hot work alloy tool steel, laser remelted or alloyed with the powders containing the NbC, TaC, TiC, VC or WC carbides based on the mass loss resulting from the abrasion wear test and the laser power used for the treatment.

The modelled artificial neural networks in which the input values are: material used for alloying, laser beam power, and the relative portions of the structural components make it possible to determine the mass loss during the abrasion wear test of the hot work alloy tool steel subjected to laser treatment.

The developed model is characteristic of the smallest average absolute error of 0.04065 for the validation set and correlation of 0.954752; for the training set the smallest average absolute error is 0.0274 and correlation is 0.977755; whereas, the smallest average absolute error in the training set is 0.04955 with the correlation equal to 0.940485. Figure 40 shows the scatter plot for

the real values in comparison with the results calculated using the artificial neural network model for the X40CrMoV5-1 hot work alloy tool steel laser remelted or alloyed with the carbides' powders, and next subjected to the abrasion wear test of the metal – ceramic material type. Figure 41 shows results of the experimental investigations which were compared with the results of tests carried out for the X40CrMoV5-1 hot work alloy tool steel laser remelted or alloyed in the laser power range of 1.2 - 2.3 kW. Prediction was made of mass loss due to the abrasion wear test in the metal-ceramic material system of the test piece from the investigated steel, which was later compared with the experimental results. The artificial neural network model response results are close to the experimental investigation results. Therefore, it is possible to use this model for predicting the abrasion wear resistance of the investigated steel after different laser surface treatments. The developed computer system features a valuable tool making it possible to carry out computer simulations of the effect of chemical composition, alloying material, and technological parameters of laser treatment on mechanical properties which eliminates the need for the time consuming experimental investigations. Therefore, it features the valuable research tool, it is used for designing the technological processes and may also find many applications in teaching as the computer assistance tool in materials engineering.

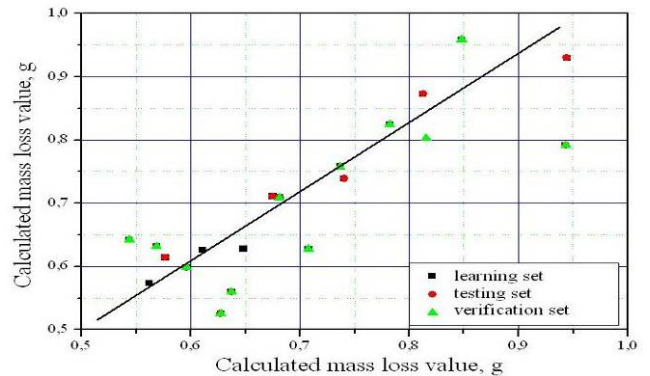


Fig. 40. Comparison of measured and calculated mass loss value using neural network model for the X40CrMoV5-1 steel

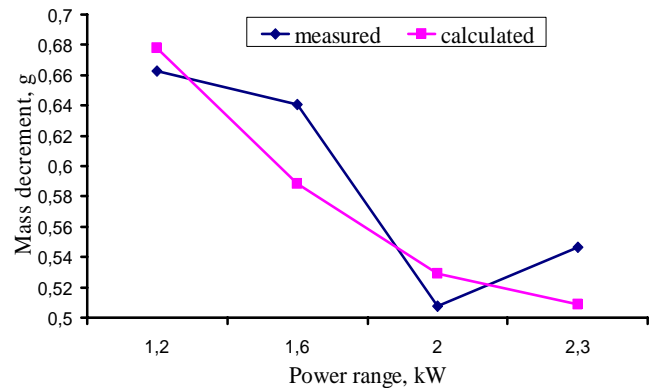


Fig. 41. Comparison of measured and calculated mass loss value using neural network model for the X40CrMoV5-1 steel alloyed using VC powder

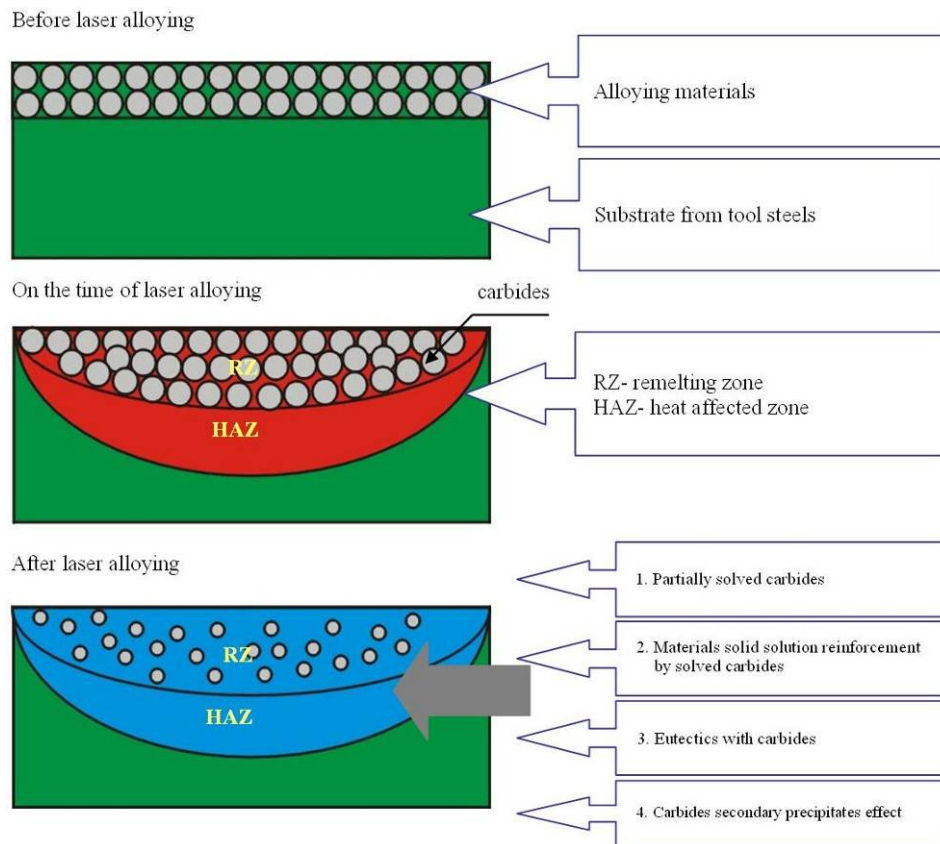


Fig. 42. Comparison of alloying additives the influence mechanism on structure and properties of the hot work tool steel surface layer

5. Summary

Examinations carried out indicate to occurrences of several mechanisms of the alloying carbides' effect on structure and properties of the surface layer of the investigated steels, depending on the dissolution extent of the alloying additives in this layer's matrix, depending both on the type of the alloying carbides used, as well as on the laser power. Figure 42 shows the general schema of the surface layer development on the investigated tool steels. The presented research results give grounds to the statement that the fabricated gradient surface layers, especially those made using the vanadium- and titanium carbides powders may be used for manufacturing new tools used for hot working. The results obtained make continuation possible of the research carried out and extend the area of interest in this problem, and especially in the laser treated steels investigations, according to criteria corresponding to the hot work tools service conditions, especially employing the thermal fatigue resistance-, hardness-, and abrasion wear resistance tests.

Acknowledgements

The research was financed partially within the framework of the research project PBZ-100/4/2004 of the Polish State Committee for Scientific Research, headed by Prof. L.A. Dobrzański.

Notice

In the framework of the subject matter described in the given paper Prof. L.A. Dobrzański gave an inaugural lecture at the 12th International Materials Symposium IMSP'2008, Pamukkale University, Denizli, Turkey taking place on 15-17.10.2008 and an invited lecture at the International Conference Advances in Materials and Processing Technologies AMPT'2008, Manama, Kingdom of Bahrain taking place on 2-11.11.2008.

References

- [1] Y. Miyamoto, W.A. Kaysser, B.H. Rabin, A. Kawasaki, R.G. Ford, *Functionally Graded Materials*, Kluwer Academic Publishers, Boston, 1999.
- [2] T. Hirai, in R.J. Brook (Ed.), *Materials Science and Technology*, Vol. 17B, *Processing of Ceramics*, Part 2, VCH Verlagsgesellschaft, Weinheim, Germany, 1996, 292-341.
- [3] A. Kawasaki, R. Watanabe, *Concept and P/M fabrication of Functionally Gradient Materials*, *Ceramics International* 23 (1997) 73-83.
- [4] B. Kieback, A. Neubrand, H. Riedel, *Processing techniques for functionally graded materials*, *Materials Science and Engineering A* 362 (2003) 81-106.

- [5] M. Yuki, T. Murayama, T. Irisawa, A. Kawasaki, R. Watanabe, in M. Yamanouchi, M. Koizumi, T. Hirai, I. Shiota (Eds.), FGM'90, Proceedings of the 1st International Symposium on Functionally Gradient Materials, Sendai, FGM Forum, Tokyo, 1990, 203-208.
- [6] W. Lengauer, K. Dreyer, Functionally graded hardmetals, *Journal of Alloys and Compounds* 338 (2002) 194-212.
- [7] E.M. Ruiz-Navas, R. Garc'ya, E. Gordo, F.J. Velasco, Development and characterisation of high-speed steel matrix composites gradient materials, *Journal of Materials Processing Technology* 143-144 (2003) 769-775.
- [8] Z. Changchi, Study of protection from cracks in laser cladding of metal- ceramic composite coating, *The International Society for Optical Engineering* 2888 (1996) 259-264.
- [9] J.H. Abboud, Functionally gradient titanium-aluminide composites produced by laser cladding, *Journal of Materials Science* 29/13 (1994) 3393-3398.
- [10] Z. Tao, Microstructures and tribological behavior of Cr/WC laser modified gradient layer on cast Al.-Si alloy, *Journal of Shanghai Jiaotong University* 36/5 (2002) 612-615.
- [11] P. Yutao, Laser clad TiC_p/Ni alloy functionally gradient coating and its in-situ formation mechanism, *Acta Metallurgica Sinica* 34/9 (1998) 987-991
- [12] W. Xiaolei, In situ formation by laser cladding of TiC composite coating with a gradient distribution, *Surface and Coatings Technology* 115/2 (1999) 111-115.
- [13] J.T.M. De Hosson, V. Ocelik, Functionally graded materials produced with high power laser, *Materials Science Forum* (2003) 163-176.
- [14] L. Qibin, Microstructure and character of friction and wear of WC_p/Ni based alloy gradient composite coating by wide-band laser cladding, *Acta Materiae Compositae Sinica* 19/6 (2002) 98-103.
- [15] Z. Tao, Microstructure of Ni/WC laser gradient coating on cast AL-Si alloy, *Journal of Shanghai Jiaotong University* 36/1 (2002) 203-208.
- [16] T. Nailing, Laser cladding high temperature alloy and WC ceramic, *The International Society for Optical Engineering* 3862 (1999) 47-55.
- [17] M. Bonek, L.A. Dobrzański, M. Piec, E. Hajduczek, A. Klimpel, Crystallisation mechanism of laser alloyed gradient layer on tool steel, *Journal of Achievements in Materials and Manufacturing Engineering* 20 (2007) 411-414.
- [18] L.A. Dobrzański, M. Piec, A. Klimpel, Z. Trojanowa, Surface modification of hot work tool steel by high-power diode laser, *International Journal of Machine Tools and Manufacture* 47/5 (2007) 773-778.
- [19] L.A. Dobrzański, M. Piec, M. Bonek, E. Jonda, A. Klimpel, Mechanical and tribological properties of the laser alloyed surface coatings, *Journal of Achievements in Materials and Manufacturing Engineering* 20 (2007) 235-238.
- [20] L.A. Dobrzański, M. Piec, A. Klimpel, Improvement of the hot work tool steel surface layers properties using a high power diode laser, *Journal of Achievements in Materials and Manufacturing Engineering* 21/1 (2007) 13-22.
- [21] L.A. Dobrzański, M. Bonek, M. Piec, E. Jonda, Diode laser modification of surface gradient layer properties of a hot-work tool steel, *Materials Science Forum* 532-533 (2006) 657-660.
- [22] M. Bonek, L.A. Dobrzański, A. Klimpel, Structure and properties of hot-work tool steel alloyed by WC carbides by a use of high power diode laser, *Journal of Achievements in Materials and Manufacturing Engineering* 24/2 (2007) 175-178.
- [23] L.A. Dobrzański, M. Piec, K. Labisz, M. Bonek, A. Klimpel, Functional properties of surface layers of X38CrMoV5-3 hot work tool steel alloyed with HPDL laser, *Journal of Achievements in Materials and Manufacturing Engineering* 24/2 (2007) 191-194.
- [24] L.A. Dobrzański, K. Labisz, M. Piec, A. Klimpel, Modelling of surface layer of the 32CrMoV12-28 tool steel using HPDL laser for alloying with TiC powder, *Journal of Achievements in Materials and Manufacturing Engineering* 24/2 (2007) 27-34.
- [25] M. Piec, L.A. Dobrzański, K. Labisz, E. Jonda, A. Klimpel, Laser Alloying with WC Ceramic Powder in Hot Work Tool Steel using a High Power Diode Laser (HPDL), *Advanced Materials Research* 15-17 (2007) 193-198.
- [26] L.A. Dobrzański, K. Labisz, A. Klimpel, Structure and properties of the laser alloyed 32CrMoV12-28 with ceramic powder, *International Journal of Surface Science and Engineering* (2007) 237-245.
- [27] L.A. Dobrzański, E. Jonda, A. Polok, A. Klimpel, Comparison of the thermal fatigue surface layers of the X40CrMoV5-1 hot work tool steels laser alloyed, *Journal of Achievements in Materials and Manufacturing Engineering* 24/2 (2007) 135-138.
- [28] L.A. Dobrzański, E. Jonda, A. Kriz, K. Lukaszowicz, Mechanical and tribological properties surface layer of the hot work tool steel obtained by laser alloying, *Archives of Materials Science and Engineering* 28/7 (2007) 389-396.
- [29] L.A. Dobrzański, A. Polok, P. Zarychta, E. Jonda, M. Piec, K. Labisz, Modelling of properties of the alloy tool steels after laser surface treatment, *International Journal of Computational Materials Science and Surface Engineering* 5 (2008) 135-147.
- [30] M. Bonek, L.A. Dobrzański, The study of properties of laser modified hot-work tool steel surface layer, *Journal of Achievements in Materials and Manufacturing Engineering* 28/1 (2008) 75-78.
- [31] M. Bonek, L.A. Dobrzański, Microstructural and tribological characterization of hot-work tool steel modified by laser alloying, *Proceedings of the 24th International Manufacturing Conference IMC24, Manufacturing – Focus on the Future, Waterford Institute of Technology, Ireland, 2007, 805-812.*
- [32] L.A. Dobrzański, K. Labisz, M. Bonek, A. Klimpel, Structure and properties of the 32CrMoV12-28 hot work tool steels alloyed with BN and Si₃N₄ powder using HPDL laser, *The International Conference Advances in Materials and Processing Technologies AMPT'2008, Manama, Kingdom of Bahrain, 2008, (CD-ROM).*
- [33] L.A. Dobrzański, K. Labisz, M. Bonek, A. Klimpel, Comparison of WC, VC and TaC powder HPDL alloyed 32CrMoV12-28 steel with using HPDL laser, *Journal of Achievements in Materials and Manufacturing Engineering* 30/2 (2008) 187-192.